Received: 30 July 2020 | Revised: 30 July 2020 | Accepted: 5 August 2020

DOI: 10.1111/ijac.13609

International Journal of Applied Ceramic Technology

ORIGINAL ARTICLE

Porous chitosan/ZnO-doped bioglass composites as carriers of bioactive peptides

Monika Biernat[1] | **Lidia Ciołek**[1] | **Maria Dzierżyńska**[2] | **Artur Oziębło**[1] | **Justyna Sawicka**[2] | **Milena Deptuła**[3] | **Marta Bauer**[4] | **Wojciech Kamysz**[4] | **Michał Pikuła**[3] | **Zbigniew Jaegermann**[1] | **Sylwia Rodziewicz-Motowidło**[2]

[1]Department of Biomaterials, Ceramic and Concrete Division, Łukasiewicz Research Network Institute of Ceramics and Building Materials, Warsaw, Poland

[2]Department of Biomedical Chemistry, Faculty of Chemistry, University of Gdansk, Gdansk, Poland

[3]Laboratory of Tissue Engineering and Regenerative Medicine, Department of Embryology, Medical University of Gdansk, Gdansk, Poland

[4]Faculty of Pharmacy, Medical University of Gdansk, Gdansk, Poland

Correspondence
Monika Biernat, Department of Biomaterials, Ceramic and Concrete Division, Łukasiewicz Research Network Institute of Ceramics and Building Materials, 02-676 Warsaw, Poland.
Email: m.biernat@icimb.pl

Funding information
Narodowe Centrum Badań i Rozwoju, Grant/Award Number: TECHMATSTRATEG2/406384/7/NCBR/2019

Abstract

In this study, we aimed to assess whether the composite of chitosan/ZnO-doped bioglass can be applied as a suitable scaffold for the incorporation of bioactive peptides. Material of a porous composite with 1:1 ratio of bioglass:polymer was produced and used as a matrix for delivery of peptide. A peptide with the PEPTIDES sequence (Pro-Glu-Pro-Thr-Ile-Asp-Glu-Ser) was chosen as a model peptide. Microstructure and pore sizes of chitosan/ZnO-doped bioglass were assessed. Open porosity and pore sizes of the composite were suitable for enabling the migration of cells and ensuring the easy delivery of nutrients within the implant. In addition, composite showed bioactivity and bactericidal activity against *Staphylococcus aureus* and *Pseudomonas aeruginosa* strains. Peptide alone did not have any cytotoxic activity on human fibroblasts and keratinocytes. Also it did not show any antibacterial properties and did not cause hemolysis of red blood cells. The peptide incorporated in composite showed a rapid release in the kinetics profile. The obtained results indicate that there is the technological possibility to incorporate peptides in chitosan/ZnO-doped bioglass scaffolds. Such biomaterials have potential application in bone tissue engineering.

KEYWORDS

bioactive glass, composites, porous materials

1 | INTRODUCTION

There is still growing worldwide interest in the development of synthetic materials for the repair and treatment of bone defects. It results from the limitations of currently used medical treatments with using as well autografts as allografts. The problems are as follows: limited supply of donor bones available for transplantation, the need for additional surgical procedures, and due to the host's immunological response triggered by the transplant.[1] Therefore, synthesizing novel biomaterials that mimic the properties to the natural extracellular matrix of the bone and applying them in the reconstructive surgery are the primary goals of the scientists and clinicians involved in the bone tissue engineering (BTE).[2-4] The success of such a biomaterial largely depends on its ability to achieve a good level of osseointegration with the host bone. This is becoming increasingly possible due to the recent advancements and technological improvements in the field of BTE.

The major components of BTE are the scaffolds, cells, and the embedded growth factors/peptides/genes for delivery.[5] It can be broadly understood that an implant should be composed of a porous degradable material known as a scaffold with suitable characteristics such as being porous; being biocompatible and bioresorbable; having suitable surface

chemistry for cell attachment, proliferation, and differentiation; and having mechanical properties that mimic the site of implantation. They should also be osteoinductive and be able to perform osteoconduction.[6,7] The ideal scaffold should have a three-dimensional structure and have the appropriate pore size and architecture. They ensure the proper retention of tissue volume, perform temporary mechanical functions, and deliver bioactive compounds, in addition to supporting flow transport of nutrients and metabolic waste.[5,8]

Considering the aforementioned properties of a scaffold, the ideal material should mimic the natural extracellular matrix of the bone; therefore polymers, such as collagen, alginate, or chitosan, have been extensively studied.[6,9] Because of its osteoconductive properties, chitosan is particularly suitable for hard tissue engineering.[10] The primary interesting characteristics of chitosan include biocompatibility and bioresorbability, intrinsic antimicrobial and hemostatic properties.[11-13] Furthermore, it can be synthesized in various forms with various geometries suitable for osteoconduction.[14-16]

The porous polymer scaffolds are often filled by hydroxyapatite particles that mimic the natural extracellular matrix of the bone.[17,18] There are also reports on the introduction of bioactive glasses into the structure of the scaffold, which increases the bioactivity of the scaffolds, thereby supporting bone regeneration.[19-21] Bioglasses are often additionally doped with elements such as silver, gold, copper, zinc, and cerium, which adds to their antibacterial properties.[20,22-27]

Another approach in BTE is the incorporation of biomimetic peptides into the scaffolds. They have recently shown great potential in obtaining new scaffolds for BTE, as an interesting alternative to expensive growth factors which are usually characterized by immunogenicity, short half-life, and not fully controlled bioactivity.[28-30] Peptides that mediate cellular adhesion or induce osteogenic differentiation of progenitor cells, as well as those that control angiogenesis to promote bone formation, have been described in literature.[9,31-34] The use of biomimetic peptides opens the way to obtain cheaper, safer, and more effective implants for bone regenerative medicine. Considering the small size of peptide molecules and the ease of their elution after in vivo administration, the origin of peptide and its interaction with the target cells should be considered in the delivery strategy of peptide molecules to/on the BTE scaffold. Therefore, the method of introducing them to the biomaterial and controlling the rate of their release is very important. One of the methods of delivery of peptides to the biomaterial structure is via adsorption of the peptides onto the surface of the biomaterial by incubating the porous scaffold in the peptide solution or by placing the peptide onto the scaffold and allowing it to dry.

Considering the advantages of polymer composites with bioactive filler and the advantages of biomimetic peptides, it seems interesting to combine such components in one material. Such a biomaterial could be potentially used in the regeneration of bone cavities, and a peptide located in polymer scaffold could promote bone tissue regeneration.

In this study, we showed a porous material composed of chitosan and ZnO-doped bioglass in which the model peptide was incorporated. The properties of the composite (eg, morphology, bioactivity, and bactericidal activity) along with the results of release tests of the model peptide from the composite were presented. We selected a peptide with good solubility in aqueous solution and with neutral biological properties so that it should not interfere with the biological properties of the composite. The peptide is stable in water and plasma so it is easily detected during the release studies without taking into the consideration its intrinsic decay properties. The current publication is the first step in the study of multicomponent composites as bone implants.

2 | EXPERIMENTAL METHODS

2.1 | Materials

In order to obtain porous composite, the following components were used: tetraethoxysilane, zinc nitrate(V) hexahydrate (Sigma-Aldrich), triethyl phosphate(V) (Fluka), calcium nitrate(V) tetrahydrate (POCH), chitosan with 74% degree of deacetylation, and 411 mPas viscosity, acetic acid (with 80% purity), and ethanol (96% p.a. grade) (POCH).

In order to obtain peptide with a PEPTIDES sequence (PPS) the following components were used: N-Fmoc-amino acids (Trimen), Rink Amide ProTide resin (CEM Corp.), Oxyma Pure (Trimen), *N,N′*-diisopropylcarbodiimide (Trimen), piperidine (Sigma-Aldrich), dimethylformamide (POCH), N-acetylimidazole (Sigma-Aldrich), triisopropylsilane (Sigma-Aldrich), trifluoroacetic acid (TFA, Iris Biotech), phenol (Sigma-Aldrich), and acetonitrile (MeCN, POCH).

2.2 | Preparation of porous chitosan-based ZnO-doped bioglass composites

Porous composites were prepared on the base of chitosan solution and ZnO-doped bioglass from $CaO\text{-}SiO_2\text{-}P_2O_5$ system. For the tests, we received bioglass by sol-gel method. In the bioglass 1 wt% of CaO was replaced with ZnO (among which 50% of the grains were below 30 μm (P5Zn1g)) or in which 2 wt% of CaO was replaced with ZnO (among which grains were smaller than 1 mm (P5Zn2)). Procedure for obtaining the composites has been mentioned in our previous work.[19] The composites were derived by means of lyophilization of stable dispersions formed by mixing of 2% chitosan

solution in acetic acid solution with bioglass grains in order to maintain 1:1, 1:3, and 1:5 bioglass and polymer weight ratios in the composites (Table 1). The lyophilization process involved freezing and sublimation of the solvent using the Christ BETA 1-16 lyophilizer.

2.3 | Characterization of porous chitosan-based ZnO-doped bioglass composites

2.3.1 | Microscopic observation

Microscopic observations of the obtained composites and composites with peptides on the surface were recorded using a scanning electron microscope with field emission (Nova NanoSEM 200, FEI). Imaging of nonsputtered samples was conducted under low vacuum conditions using vCD detector at 15 kV accelerating voltage. Nonmodel chemical analysis involving superficial effects after incubation of composites in a simulated body fluid (SBF) and under low vacuum conditions was performed using an energy-dispersive X-ray spectroscopic (EDS) detector, SDD Apollo X model, EDAX. However, imaging of sample's microstructure was performed under high vacuum conditions using an Everhart–Thornley detector (ETD) at 10 kV accelerating voltage. Before the study, the samples were covered with conductive material (10 nm gold film) using a sputter coater (Leica EM SCD500). Macropore sizes of the obtained composites were determined on the basis of microscopic images using measurement and annotation functions on the sample area.

2.3.2 | Bioactivity tests

The obtained composites were subjected to bioactivity tests by the methods described previously.[19] In brief, the samples were placed in sealed glass vessels containing SBF[35] and were stored in a dryer at 37°C for 28 days. SBF was exchanged every 7 days. After 28 days, the samples were removed, rinsed with distilled water, dried in a lyophilizer, and subjected to SEM-EDS analysis.

2.3.3 | Specific surface area analysis

As in our previous work,[19] the specific surface area of samples was measured by Brunauer, Emmett, and Teller (BET) method using nitrogen adsorption at −195.8°C with Quadrasorb-SI instrument, Quantachrome. Before the measurements were taken, the samples were degassed for 24 hours at 150°C. The volume and pore sizes of the samples was measured based on the experimentally designated physical nitrogen sorption isotherms. Distributions of pore sizes of the studied composites were obtained based on the experimentally designated physical nitrogen desorption isotherms using Barret, Joyner, and Halend (BJH) method.

2.4 | Peptide synthesis

The peptide was synthesized with Liberty Blue™ Automated Microwave Peptide Synthesizer on the Rink Amide ProTide resin—Fmoc solid-phase peptide synthesis. The purity of the synthesized compound was confirmed by analytical reverse phase high-performance liquid chromatography (RP-HPLC) photodiode array (PDA) detector and the low-temperature evaporative light-scattering detector (ELSDLT-II). The counter ion was exchanged to the acetate on micro-column with a strong cation exchanger. The peptide mass was confirmed by liquid chromatography mass spectrometry-ion trap-time-of-flight (LCMS-IT-TOF).

2.5 | Peptide characterization

2.5.1 | Stability in water and plasma

Peptide PEPTIDES (final concentration of 107 μmol/L) was incubated in plasma for 24 hours at 37°C and the samples were collected at 0, 1, 2, 3, 6, and 24 hours time points. The samples were also prepared in water and incubated in the same conditions. After the appropriate time, fourfold excess of absolute ethanol (v/v) was added and samples were centrifuged (32,000 rcf; 4°C; 20 minutes). The supernatant was collected, air-dried under vacuum, and dissolved in 0.01% TFA in H_2O. HPLC

TABLE 1 Composites obtained using bioglass and chitosan

Bioglass type	Weight ratio - bioglass: polymer	Composite marking	Macropore size range[a] [μm]
Bioglass P5Zn1g	1:1	P5Zn1gCh_1:1	40-90
	1:3	P5Zn1gCh_1:3	50-120
	1:5	P5Zn1gCh_1:5	70-120
Bioglass P5Zn2	1:1	P5Zn2Ch_1:1	40-110

[a]Determined on the basis of microscopic images with using measurement and annotation functions on the sample area.

(Phenomenex Luna C18(2) (5 μm, 100 Å 4.6 × 250 mm) column) was performed using 0.01% TFA in H_2O (A) and 0.01% TFA in 80% MeCN in water (B) as solvents. A linear gradient of 5%–100% in 60 minutes and a flow rate of 1 mL/min was applied. For calculations, peak areas were compared to a calibration curve calculated by Shimadzu LCSolution Software. Experiments were performed in triplicate, and the results were expressed as mean ± standard deviation (SD).

2.5.2 | Peptide cytotoxicity

Two types of cells were used in the study: human immortalized human HaCaT keratinocytes (DKFZ Heidelberg, Germany) and human dermal fibroblasts cell line 46BR.1N (European Collection of Cell Cultures (ECACC), Sigma-Aldrich). HaCaT cells are spontaneously immortalized human keratinocytes. They maintain most of the normal human keratinocytes functions including, for example, the expression of major surface markers, differentiation potential or response to different stimuli.[36-38] 46BR.1N cells were originally derived from the skin of individual with hypogammaglobulinemia and immortalized by transformation with the plasmid pSV3neo.[39] Cells were grown in Dulbecco's modified Eagle's medium (DMEM) supplemented with 4500 mg/L of glucose, 584 mg/L of L-glutamine, sodium pyruvate, and sodium bicarbonate containing 10% fetal bovine serum (FBS), 100 units/mL of penicillin, and 100 μg/mL of streptomycin (all Sigma-Aldrich Co., USA). The cells were routinely cultured under a humidified atmosphere with 5% CO_2 at 37°C in culture flasks (growth surface area of 25 cm^2).

For the cytotoxicity analysis, cells were seeded into 96-well plates (5000 cells per well) in DMEM with high glucose content (4500 mg/L, DMEM HG) containing 10% FBS. After 24 hours, the medium was changed to serum-free DMEM, and the cells were stimulated with appropriate concentrations of PPS prepared with water under sterile conditions. After 48 hours of incubation, cell culture supernatants were collected and lactate dehydrogenase (LDH) assay (Takara, Japan, cat. No. MK401) was performed according to manufacturer's recommendations. Non-PPS-treated cells were used as negative control (0%) and Triton-X 100 (1%) was used as the positive control for maximum LDH release (maximum cytotoxicity, 100%).

2.5.3 | Antimicrobial and hemolysis assay

Minimal inhibitory concentrations (MICs) were determined by the broth microdilution method according to the recommendations provided by the Clinical and Laboratory Standards Institute (CLSI).[40,41] The activity of peptide was determined for reference strains of microorganisms: *Staphylococcus aureus* ATCC 25923, *Staphylococcus epidermidis* ATCC 14990, *Escherichia coli* ATCC 25922, *Pseudomonas aeruginosa* ATCC 9027, and *Candida albicans* ATCC 10231. Briefly, the initial inoculums of bacteria (5×10^5 CFU/mL) in Mueller-Hinton Broth and fungi (2×10^3 CFU/mL) in RPMI-1640 were exposed to the concentrations of the peptide ranging from 1 to 512 μg/mL. Bacteria and fungi were incubated at 37°C for 18 and 24 h, respectively. The MIC was defined as the lowest peptide concentration with no visible growth of bacteria and fungi. The experiment was performed in triplicate.

For hemolysis assay,[42] fresh human blood with ethylenediaminetetraacetic acid (EDTA) as the anticoagulant was rinsed three times with PBS by centrifugation at 800× *g* for 10 minutes to obtain RBCs without serum and then cells were resuspended in PBS. Peptide solution was serially diluted in PBS on 96-well plates to obtain concentrations ranging from 1 to 512 μg/mL. Then, the stock solution of RBCs was added to reach a final volume of 100 μL with a 4% concentration of erythrocytes (v/v). The control wells for 0 and 100% hemolysis consisting of RBCs suspended in PBS and 1% of Triton-X 100, respectively, were also prepared. Subsequently, the plates were incubated for 60 minutes at 37°C and then centrifuged at 800× *g* for 10 minutes at 4°C. After centrifugation, the supernatant was carefully transferred to new microtiter plates and the hemoglobin released was measured at 540 nm. Hemolysis was expressed as the percentage amount of hemoglobin released compared with well with 100% hemolysis.

2.6 | Incorporation of the peptide into the porous composite

The selected peptide with a PEPTIDES sequence was incorporated into one of the obtained composites by dipping the composite sample into the 0.1 mg/mL peptide solution for 12 hours at 4°C and subsequent lyophilization. This procedure and method of drying ensure the maintenance of unchanged properties of ingredients of biocomposites.

2.7 | Peptide release from porous composite

Chitosan-based ZnO-doped bioglass composite with absorbed peptide was immersed in 25 mL of receiving solution (phosphate-buffered saline (PBS)). The solution was kept in an incubator (32°C) and stirred for 24 hours. Samples (100 μL) were withdrawn at several time points during 27 hours, substituting each one with 100 μL of fresh PBS solution. Samples were frozen at −20°C. After the incubation, the solvent was removed on a speedvac, and the samples were dissolved in 110 μL MiliQ water. HPLC was performed by applying the same column, solvents, and calculations as given in Section 4.5.1.

2.8 | Bactericidal activity of chitosan-based ZnO-doped bioglass composites

According to the method described in our previous article,[20] the composites were subjected to the antibacterial tests against *P aeruginosa* and the *S aureus* strains. The in vitro tests of bactericidal properties were performed by means of the dilution method. Briefly, precultures of the bacterial strains were incubated in a nutrient broth at 37°C ± 1°C for up to 18-20 hours. Samples of the composites were presterilized by UV exposure for 45 minutes at room temperature, and then the samples were inserted into the wells of a 24-well plate (Nunc). To this, 1 mL of bacterial culture was added. The solutions were incubated for 24, 48, 72 hours, and 7 days, after which 100 μL of each bacterial culture was collected, diluted with 0.9% NaCl, and plated out on nutrient agar. The plates were incubated at 37°C ± 1°C for 24 hours, and then the colonies were counted. Broth cultures of microorganisms without the biomaterials served as controls. All the tests were performed in triplicate.

2.9 | Statistical analysis

Statistical significance in cytotoxicity assay was determined with the Mann-Whitney *U*-test ($P < .05$) in STATISTICA StatSoft Polska, Krakow, Poland).

3 | RESULTS

3.1 | Properties of porous chitosan/ZnO-doped bioglass composites

The porous chitosan/ZnO-doped bioglass composites obtained by liquid dispersion lyophilization were considered as the matrix for the incorporation of model peptide. The microstructure of the composites was controlled by the appropriate content of bioglass in relation to the polymer content and by the grain size of glass.[19] The chemical formulations of bioglass fitted $CaO\text{-}SiO_2\text{-}P_2O_5$ system. Bioglass of 70 wt% SiO_2, 5 wt% P_2O_5, and 25 wt% CaO was used as a reference material. In the composition of ZnO-doped bioglass 1 wt% or 2 wt% CaO was replaced with ZnO. The obtained P5Zn2 glass powder contained grains smaller than 1 mm and the obtained P5Zn1g glass powder was reground and 50% of its grains was below 30 μm.[19] Depending on the grain size of the glass and the ratio of bioglass/chitosan, the obtained composites were characterized by various macropore sizes in the range of 40-120 μm (Table 1). The obtained composites were highly porous and the pores were found to be open and internally connected. Composites with bioglass:polymer weight ratio equal 1:1 showed the most regular and undisrupted microstructure. Figure 1 shows an SEM image of the cross-sections of one of the obtained composites—P5Zn1gCh_1:1. Their porosity determined by the BET method showed that d_{BJH} was at 3 nm, which indicates the presence of micro and mesopores in the composite.

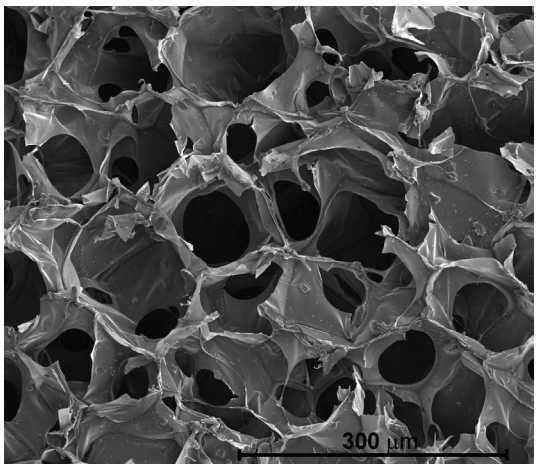

FIGURE 1 SEM image of composite chitosan/ZnO-doped bioglass P5Zn1gCh_1:1

An important feature of biomaterials for bone tissue regeneration is also bioactivity, which can be determined by the ability to induce the growth of a layer similar to the bone component—hydroxyapatite. Our observation of changes in the intensity of Si, Ca, and P signals on the EDS spectra of the composite revealed the slow formation of the apatite layer (Figure 2). The bioactivity-inducing component in the obtained composites is mainly bioglass particles.

An additional advantage of the studied composites is their effect on microorganisms. Our previous in vitro research show that the considered chitosan/ZnO-doped bioglass composites are not cytotoxic.[20] In cytotoxicity tests conducted by the method of direct contact of the mouse fibroblast line L929 (American Type Culture Collection Certified Cell Line-ATCC CCL1) no hazardous substances were released from these composites during an extraction process.[20]

Moreover for two selected from Table 1 composites, which microstructure was the most regular, bactericidal activity tests were carried out. The considered composites were prepared with the bioglass:polymer weight ratio equal 1:1, with various ZnO content in bioglass and various grain size of bioglass (P5Zn2Ch_1:1, P5Zn1gCh_1:1). As intended the antibacterial properties of our composites were associated with the presence of ZnO, and their antibacterial mechanism was fully discussed in previous works.[20,43-45] The obtained results indicated the antibacterial activity of the tested composites against *S aureus* and *P aeruginosa* strains (Figure 3). The tested composites more clearly inhibited the growth of the *S aureus* strain. After 24 hours of contact with

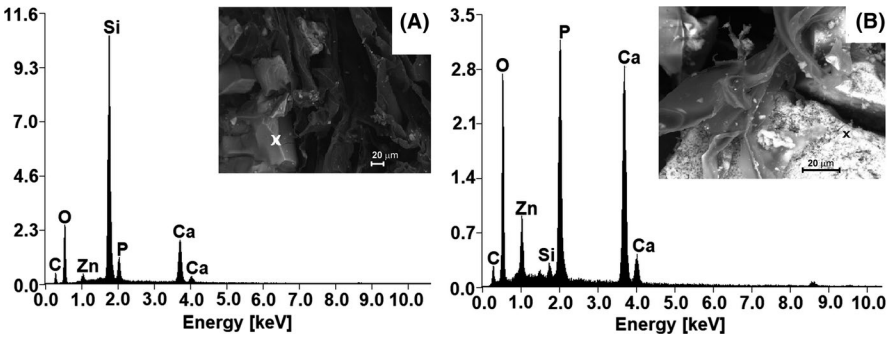

FIGURE 2 Energy-dispersive X-ray spectroscopic (EDS) analyses within bioglass area of P5Zn2Ch_1:1 composite and scanning electron microscopic (SEM) images before (A) and after (B) incubation in simulated body fluid (SBF)

S aureus, the higher antibacterial activity was demonstrated by the composite containing bioglass enriched by 2 wt% of Zn (P5Zn2Ch_1:1). However after 48 hours, when the number of cells in control cultures was the highest, the activity of the composites containing of bioglass enriched with 1 wt% of Zn (P5Zn1gCh_1:1) increased significantly to the same level as composites containing of bioglass enriched with 2 wt% of Zn (P5Zn2Ch_1:1). Considering that the glass enriched with 1 wt% of Zn had a smaller grain size than that of the glass enriched with 2 wt% of Zn, it can be assumed that specific surface area of bioglass grains has a significant effect on antibacterial properties what is related to the level of bactericidal agent release over time. The antibacterial activity of the composites depended on the ZnO content of bioglass, bioglass grain size, and composite microstructure, which may be controlled via their production process parameters.

Taking into account the antibacterial activity, the microstructure of composites and the observation that composites based on finely ground bioglass (grains below 30 μm) with the highest (1:1) bioglass/polymer ratio were characterized by the greatest structural stability, the composite P5Zn1gCh_1:1 was selected to conduct further research as carrier of bioactive peptides.

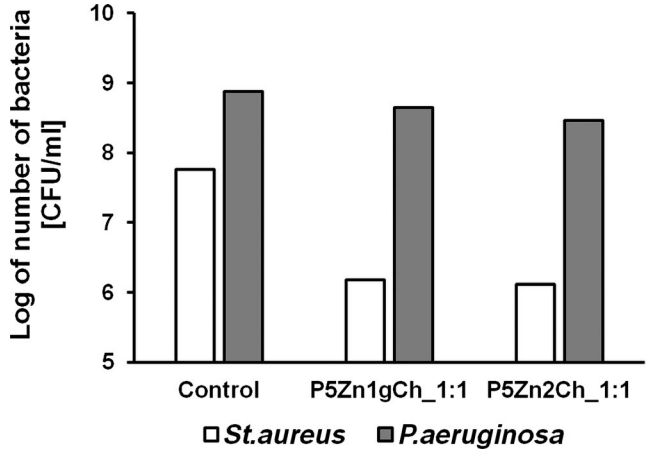

FIGURE 3 Viability of strains determined after 48 h contact of *Staphylococcus aureus* and *Pseudomonas aeruginosa* with the composites P5Zn1gCh_1:1 and P5Zn2Ch_1:1

3.2 | Properties of the model peptide

The peptide with a PEPTIDES sequence was selected as a model peptide. Its most important properties (stability in water and plasma) which are crucial during release studies were investigated.

The first experiment was to determine the stability of the peptide in water. Its decay might influence the release kinetics of the peptide from the composite. Incubation of PPS peptide in water and plasma indicated that the compound is stable in both conditions (Figure 4). It is not susceptible to the components of human plasma (eg, enzymes) and probably does not bind to albumins.

PPS peptide was not cytotoxic to either human keratinocytes or dermal fibroblast (Figure 5). Moreover, the XTT test showed that PPS peptide stimulates the proliferation of HaCaT cells at concentrations ranging from 0.1 to 25 μg/mL (20%–30% increase in proliferation compared to the non-PPS-treated control; Figure 6A) and 46BR.1N fibroblasts at concentrations ranging from 1 to 50 μg/mL (10%–30% increase in proliferation compared to the non-PPS-treated control; Figure 6B). In addition, to a small extent (about 10%–15%), it inhibits the proliferation of both tested cell lines at the lowest concentration (0.01 μg/mL).

It did not either show antibacterial (*S aureus*, *S epidermidis*, *E coli*, *P aeruginosa*) and antifungal (*C albicans*) activity at the tested concentrations (1-512 μg/mL) and did not cause hemolysis of human red blood cells (data not shown).

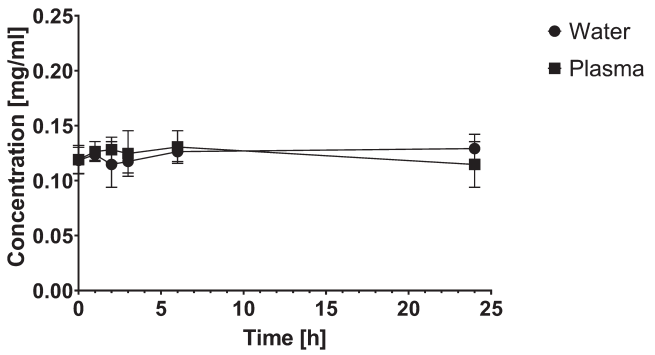

FIGURE 4 PPS stability in water and in plasma during 24 h incubation

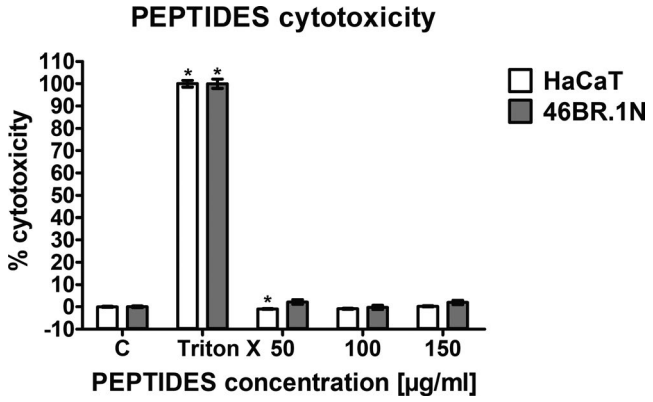

FIGURE 5 PPS cytotoxicity against human immortalized HaCaT keratinocytes and human dermal 46BR.1N fibroblasts. Graph presents mean ± standard error of mean (SEM) from three independent experiments (four replicates each). *—statistically significant differences (Mann-Whitney *U*-test, $P < .05$, n = 12) compared to negative control (non-PPS treated cells). Triton-X—positive control (maximum LDH release = maximum cytotoxicity)

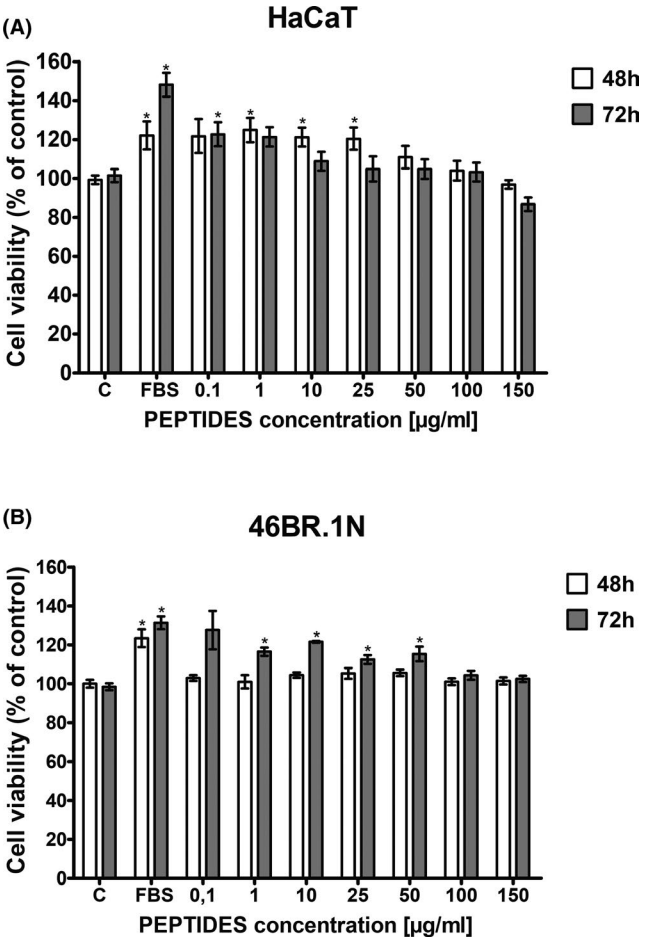

FIGURE 6 PPS effect on proliferation of human immortalized HaCaT keratinocytes (A) and dermal 46BR.1N fibroblasts (B). Graphs present mean ± standard error of mean (SEM) from three independent experiments (four replicates in each). *—statistically significant differences (Mann-Whitney *U*-test, $P < .05$, n = 12) compared to negative control. FBS-positive control (Cells grown in medium supplemented with 10% FBS)

3.3 | Incorporation of the model peptide into the porous composite and peptide release assay

The simplest strategy for introducing a peptide into a porous scaffold is via the adsorption of peptides onto the surface of the biomaterial by simply incubating the scaffold in the peptide solution. In this study, PPS peptide was incorporated into the selected porous composite (P5Zn1gCh_1:1) by dipping it into the peptide solution. After dipping and lyophilization, the microstructure of the porous composite did not change (Figure 7). Adsorption of peptides onto the surface of the chitosan/ZnO-doped bioglass composite had no effect on the pore size (the diameter and thickness of the pores remained unchanged). The image of SEM at higher magnification shows mutual communication between the pores.

After introducing the peptide into the porous biomaterial, we verified the level of peptide released from the composite scaffold. The HPLC results show a rapid initial release of peptide within the first hour (burst effect) from the porous scaffold (Figure 8). Then, the saturation of the peptide in solution was observed, represented by the presence of the plateau on a diagram. The peptide did not lose its physicochemical properties after release. Such a rapid release of the peptide may be the desired effect in the case of its antibacterial properties because it can locally, quickly, and effectively inhibit bacterial growth.

4 | DISCUSSION

Biomaterials for bone tissue regeneration must meet specific requirements so that they can support the physiological processes. Biocompatibility, bioactivity, osteoconductivity, and porosity appear to be of key importance.[5-8] With regard to bone tissue implants, the osteoinductive, osteoconductive properties, and porosity appear to be of key importance. It is assumed that the distribution and the size of pores should enable appropriate migration of cells and ensure the easy delivery of nutrients within the implant. The optimal average pore size of a scaffold should be within the range of 50-400 µm.[46] Another essential feature of an implant is its biodegradability/bioresorbability—ability to show controlled degradation and appropriate resorption to match the cellular growth with that of the site of reconstruction.

In this study, the tested biocomposites showed bioactivity and bactericidal activity. They contained bioglass enriched with Zn in their composition, which according to the literature increases the bioactivity of biomaterials.[47] ZnO added to the chemical composition of bioglass ensures also

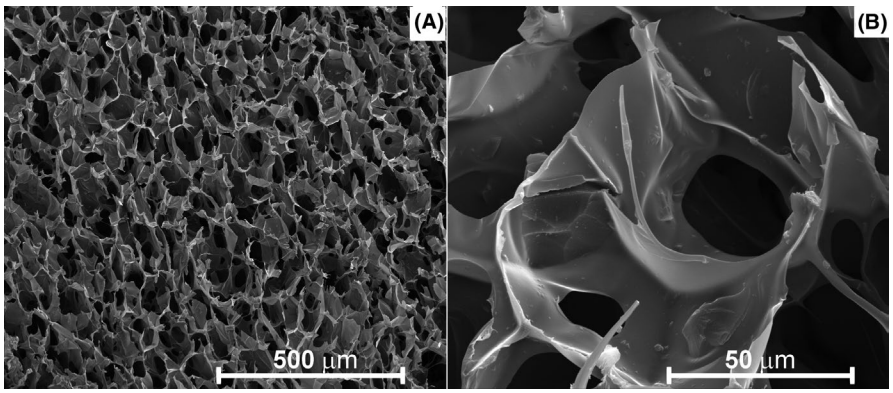

FIGURE 7 Scanning electron microscopic (SEM) image of microstructure of chitosan/ZnO-doped bioglass composite with peptide adsorbed; (A) magnification of 250×, (B) magnification of 2500×

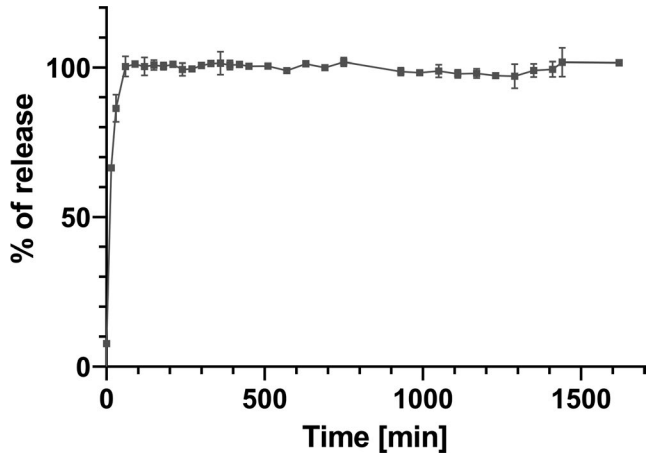

FIGURE 8 The level of peptide release from the chitosan/ZnO-doped bioglass composite

bactericidal effects of the composite.[20] According to literature data the selected composite's pore sizes were favorable for new bone tissue ingrowth.[7] Micro and mesopores are important in adsorption processes while macropores play the role of transport routes enabling the access to pores of smaller sizes. The selected composite's microstructure was then suitable for enabling the migration of cells and ensuring delivery of nutrients. It was also assumed that the selected composite can act as a carrier of peptides. PPS peptide itself is soluble in aqueous solution, stable in water and plasma, which makes it adequate material for releasing studies, eliminating decay and interfering processes. Additionally it was investigated PPS peptide is no cytotoxic and has no additional antibacterial properties. It is known that certain peptides can be cytotoxic to human cells, and therefore it was important to analyze PPS effect on human cells.[48] As an experimental model for this study we chose human immortalized cell lines: HaCaT keratinocytes and 46BR.1N fibroblasts. They are a common model used in the preliminary assessment of the toxicity of bioactive compounds, including peptides. The cells used in our study have different origin (ectodermal for keratinocytes and mesodermal for fibroblasts) and therefore may respond differently to stimulation. Besides, the use of immortalized cell lines, which maintain functions of normal cells, allows to obtain reliable and reproducible results and avoid donor-to-donor variability characteristic for primary cell cultures.[38,49-52]

Due to the porous structure of the obtained composite, we decided to combine it with the model peptide by the method of adsorption. Adsorption is especially applicable to bone morphogenetic protein (BMP)-derived peptides because the initial osteogenic stimulation of osteoprogenitor cells is important to induce the process of bone formation. The osteogenic process can then evolve autonomously by the cytokines produced by its own cells. The adsorption method allowed us to successfully introduce the peptide into the composite material and then we verify the release kinetics. The results of release kinetics of the peptide from the composite matrix are consistent with the literature. The adsorption method of peptide introduction onto the polymer scaffold usually results in a rapid, massive release of peptide molecules; therefore, it is suitable only for certain peptides derived from soluble growth factors. The reduction in the rate of release of the peptide can be achieved by incorporating the peptides into the biomaterial structure at the stage of scaffold synthesis. During the degradation progress of such a biomaterial, new peptides are still being released from its surface, leading to more long-term stimulation of resident cells. There are reports[53] on the use of a combination of both of the aforementioned methods, which may ensure greater complementarity of the activity. For example, a peptide with osteoinductive effects can be adsorbed on the implant surface, whereas an angiogenic peptide can be built into the structure of the implant. If more precise control of the release of peptides is needed, then a covalent bond[54] or somewhat weaker binding by specific domains can be used.[9,55,56]

5 | CONCLUSIONS

The results of this study indicate that the porous chitosan-based ZnO-doped bioglass composite is suitable to be used as

a scaffold for bioactive peptides. There is the technological feasibility of the location of different peptides in this composite. The selected composite did not damage the peptide during contact with it and the peptide did not lose its physicochemical properties after release. Considering the short time of the release of the peptide from the selected composite, we are planning to place slow-release peptides in the polymer scaffold or incorporate peptides by the other method than adsorption in further studies.

ACKNOWLEDGMENT

This research was funded by The National Centre for Research and Development, Poland, grant No. TECHMATSTRATEG2/406384/7/NCBR/2019

ORCID

Monika Biernat https://orcid.org/0000-0002-5692-0653
Lidia Ciołek https://orcid.org/0000-0001-5906-7195
Maria Dzierżyńska https://orcid.org/0000-0003-0861-2514
Justyna Sawicka https://orcid.org/0000-0002-1506-3202

REFERENCES

1. Laurencin C, Khan Y, El-Amin SF. Bone graft substitutes. Expert Rev Med Devices. 2006;3:49–57.
2. Venkatesan J, Bhatnagar I, Manivasagan P, Kang KH, Kim SK. Alginate composites for bone tissue engineering: a review. Int J Biol Macromol. 2015;72:269–81.
3. Burdick JA, Mauck RL. Biomaterials for tissue engineering applications. A review of the past and future trends. Wien, Germany: SpringerWienNewYork; 2011.
4. Arrabal PM, Visser R, Santos-Ruiz L, Becerra J, Cifuentes M. Osteogenic molecules for clinical applications: improving the BMP-collagen system. Biol Res. 2013;46:421–9.
5. Hollister SJ. Porous scaffold design for tissue engineering. Nat Mater. 2005;4:518–24.
6. Li Y, Ramay HR, Hauch KD, Xiao D, Zhang M. Chitosan-alginate hybrid scaffolds for bone tissue engineering. Biomaterials. 2005;26:3919–28.
7. Biano F, Fiume E, Barberi J, Kargozar S, Marchi J, Massera J, et al. Processing methods for making porous bioactive glass-based scaffolds – A state-of-the-art review. Int J Appl Ceram Technol. 2019;16:1762–96.
8. Hutmacher DW. Scaffolds in tissue engineering bone and cartilage. Biomaterials. 2000;21:2529–43.
9. Visser R, Arrabal PM, Santos-Ruiz L, Fernandez-Barranco R, Becerra J, Cifuentes M. A collagen-targeted biomimetic RGD peptide to promote osteogenesis. Tissue Eng Part A. 2014;20:34–44.
10. Sivashankari PR, Prabaharan M. Prospects of chitosan based scaffolds for growth factor release in tissue engineering. Int J Biol Macromol. 2016;93:1382–9.
11. Yilmaz AH. Antibacterial Activity of Chitosan-Based Systems. In: Jana S, Jana S, editors. Functional Chitosan. Singapore: Springer; 2019. https://doi.org/10.1007/978-981-15-0263-7_15
12. Raafat D, Bargen KV, Haas A, Sahl HG. Insights into the mode of action of chitosan as an antibacterial compound. Appl Environ Microbiol. 2008;74:3764–73.
13. Rabea EI, Badawy MET, Stevens CV, Smagghe G, Steurbaut W. Chitosan as antimicrobial agent: applications and mode of action. Biomacromol. 2003;4:1457–65.
14. Di Martino A, Sittinger M, Risbud MV. Chitosan: a versatile biopolymer for orthopedic tissue-engineering. Biomaterials. 2005;26:5983–90.
15. Wang J, Wang L, Yu H, Zain-ul-Abdin CY, Chen Q, et al. Recent progress on synthesis, property and application of modified chitosan: an overview. Int J Biol Macromol. 2016;88:333–44.
16. SionkowskaA KB, Lewandowska K, Grabska S, Pokrywczyńska M, Kloskowski T, et al. 3D composites based on the blends of chitosan and collagen with the addition of hyaluronic acid. Int J Biol Macromol. 2016;89:442–8.
17. Turco G, Marsich E, Bellomo F, Semeraro S, Donati I, Brun F, et al. Alginate/hydroxyapatite biocomposite for bone ingrowth: a trabecular structure with high and isotropic connectivity. Biomacromol. 2009;10:1575–83.
18. Senatov F, Anisimova N, Kiselevskiy M, Kopylov A, Tcherdyntsev V, Maksimkin A. Polyhydroxybutyrate/hydroxyapatite highly porous scaffold for small bone defects replacement in the non-load-bearing parts. J Bionic Eng. 2017;14:648–58.
19. Ciołek L, Biernat M, Jaegermann Z, Tymowicz-Grzyb P, Taźbierski P, Jastrzębska A, et al. Controlling the microstructure of lyophilized porous biocomposites by the addition of ZnO-doped bioglass. Int J Appl Ceram Technol. 2017;14:1107–16.
20. Ciołek L, Biernat M, Jaegermann Z, Zaczyńska E, Czarny A, Jastrzębska A, et al. The studies of cytotoxicity and antibacterial activity of composites with ZnO-doped bioglass. Int J Appl Ceram Technol. 2019;16:541–51.
21. Douglas TEL, Dziadek M, Gorodzha S, Liskova J, Barckman G, Vanhoorne V, et al. Novel injectable gellan gum hydrogel composites incorporating Zn- and Sr-enriched bioactive glass microparticles: High-resolution X-ray microcomputed tomography, antibacterial and in vitro testing. J Tissue Eng Regen Med. 2018;12:1313–26.
22. Balamurugan A, Balossier G, Laurent-Maquin D, Pina S, Rebelo AH, Faure J, et al. An in vitro biological and anti-bacterial study on a sol-gel derived silver-incorporated bioglass system. Dent Mater. 2008;24:1343–51.
23. Zhu H, Hu C, Zhang F, Feng X, Li J, Liu T, et al. Preparation and antibacterial property of silver-containing mesoporous 58S bioactive glass. Mater Sci Eng C. 2014;42:22–30.
24. Kim TN, Feng QL, Kim JO, Wu J, Wang H, Chen GC, et al. Antimicrobial effects of metal ions (Ag^{+}, Cu^{2+}, Zn^{2+}) in hydroxyapatite. J Mater Sci Mater Med. 1998;9:129–34.
25. Cui Y, Zhao Y, Tian Y, Zhang W, Lü X, Jiang X. The molecular mechanism of action of bactericidal gold nanoparticles on Escherichia coli. Biomaterials. 2012;33:2327–33.
26. Goh YF, Alshemary AZ, Akram M, Kadir MRA, Hussain R. In-vitro characterization of antibacterial bioactive glass containing ceria. Ceram Int. 2014;40:729–37.
27. Hoppe A, Güldal NS, Boccaccini AR. A review of the biological response to ionic dissolution products from bioactive glasses and glass-ceramics. Biomaterials. 2011;32:2757–74.
28. Woo EJ. Adverse events after recombinant human BMP2 in nonspinal orthopaedic procedures. Clin Orthop Relat Res. 2013;471:1707–11.
29. Hwang CJ, Vaccaro AR, Lawrence JP, Hong J, Schellekens H, Alaoui-Ismaili MH, et al. Immunogenicity of bone morphogenetic proteins. J Neurosurg Spine. 2009;10:443–51.

30. Oryan A, Alidadi S, Moshiri A, Bigham-Sadegh A. Bone morphogenetic proteins: a powerful osteoinductive compound with non-negligible side effects and limitations. BioFactors. 2014;40(5):459–81.
31. Pierschbacher MD, Ruoslahti E. Cell attachment activity of fibronectin can be duplicated by small synthetic fragments of the molecule. Nature. 1984;309:30–3.
32. Bilem I, Chevallier P, Plawinski L, Sone ED, Durrieu MC, Laroche G. RGD and BMP-2 mimetic peptide crosstalk enhances osteogenic commitment of human bone marrow stem cells. Acta Biomater. 2016;36:132–42.
33. Kanczler JM, Oreffo RO. Osteogenesis and angiogenesis: the potential for engineering bone. Eur Cell Mater. 2008;15:100–14.
34. Van Hove AH, Benoit DS. Depot-based delivery systems for pro-angiogenic peptides: a review. Front Bioeng Biotechnol. 2015;3:102.
35. Kokubo T, Takadama H. How useful is SBF in predicting in vitro bone bioactivity? Biomaterials. 2006;27:2907–15.
36. Boukamp P, Petrussevska RT, Breitkreutz D, Hornung J, Markham A, Fusenig NE. Normal keratinization in a spontaneously immortalized aneuploid human keratinocyte cell line. J Cell Biol. 1988;106:761–71.
37. Boukamp P, Popp S, Altmeyer S, Hülsen A, Fasching C, Cremer T, et al. Sustained nontumorigenic phenotype correlates with a largely stable chromosome content during long-term culture of the human keratinocyte line HaCat. Genes Chromosom Cancer. 1997;19:201–14.
38. Barańska-Rybak W, Pikuła M, Dawgul M, Kamysz W, Trzonkowski P, Roszkiewicz J. Safety profile of antimicrobial peptides: Camel, citropin, protegrin, temporin a and lipopeptide on hacat keratinocytes. Acta Pol Pharm Drug Res. 2013;70:795–801.
39. Deptuła M, Karpowicz P, Wardowska A, Sass P, Sosnowski P, Mieczkowska A, et al. Development of a peptide derived from platelet-derived growth factor (PDGF-BB) into a potential drug candidate for the treatment of wounds. Adv Wound Care. 2019. https://doi.org/10.1089/wound.2019.1051
40. Clinical and Laboratory Standards Institute (CLSI). Reference method for broth dilution antifungal susceptibility testing of yeasts. Approved Standards-Second Edition, in CLSI document M27–2A 2002, Pennsylvania, USA: CLSI; 2002.
41. Clinical and Laboratory Standards Institute (CLSI). Methods for dilution antimicrobial susceptibility tests for bacteria that grow aerobically. Approved Standard—Ninth Edition. In CLSI document M07–A9, Pennsylvania, USA: CLSI; 2012.
42. Avrahami D, Shai Y. A new group of antifungal and antibacterial lipopeptides derived from non-membrane active peptides conjugated to palmitic acid. J Biol Chem. 2004;279:12277–85.
43. Kumar R, Umar A, Kumar G, Nalwa HS. Antimicrobial properties of ZnO nanomaterials: a review. Ceram Int. 2017;43:3940–61.
44. Li M, Zhu L, Lin D. Toxicity of ZnO Nanoparticles to escherichia coli: mechanism and the influence of medium components. Environ Sci Technol. 2011;45:1977–83.
45. Sirelkhatim A, Mahmud S, Seeni A, Kaus NHM, Ann LC, Bakhori SKM, et al. Review on zinc oxide nanoparticles: antibacterial activity and toxicity mechanism. Nano-Micro Lett. 2015;7:219–42.
46. Kim BS, Park IK, Hoshiba T, Jiang HL, Choi YJ, Akaike T, et al. Design of artificial extracellular matrices for tissue engineering. Prog Polym Sci. 2011;36:238–68.
47. Thian ES, Konishi T, Kawanobe Y, Lim PN, Choong C, Ho B, et al. Zinc-substituted hydroxyapatite: a biomaterial with enhanced bioactivity and antibacterial properties. J Mater Sci Mater Med. 2013;24:437–45.
48. Deptuła M, Wardowska A, Dzierżyńska M, Rodziewicz-Motowidło S, Pikuła M. Antibacterial peptides in dermatology-strategies for evaluation of allergic potential. Molecules. 2018;23:414.
49. Kosikowska P, Pikuła M, Langa P, Trzonkowski P, Obuchowski M, Lesner A. Synthesis and evaluation of biological activity of antimicrobial pro-proliferative peptide conjugates. PLoS One. 2015;10:1–16.
50. Dębowski D, Łukajtis R, Łęgowska A, Karna N, Pikuła M, Wysocka M, et al. Inhibitory and antimicrobial activities of OGTI and HV-BBI peptides, fragments and analogs derived from amphibian skin. Peptides. 2012;35:276–84.
51. Sass P, Sosnowski P, Podolak-Popinigis J, Górnikiewicz B, Kamińska J, Deptuła M, et al. Epigenetic inhibitor zebularine activates ear pinna wound closure in the mouse. EBioMedicine. 2019;46:317–29.
52. Skowron P, Krawczun N, Żebrowska J, Kreft D, Zolnierkiewicz O, Bielawa M, et al. A vector-enzymatic DNA fragment amplification-expression technology for construction of artificial, concatemeric DNA, RNA and proteins for novel biomaterials, biomedical and industrial applications. Mater Sci Eng C. 2020;108:110426.
53. Geuze RE, Theyse LFH, Kempen DHR, Hazewinkel HAW, Kraak HYA, Öner FC, et al. A differential effect of bone morphogenetic protein-2 and vascular endothelial growth factor release timing on osteogenesis at ectopic and orthotopic sites in a large-animal model. Tissue Eng Part A. 2012;18:2052–62.
54. Maia FR, Bidarra SJ, Granja PL, Barrias CC. Functionalization of biomaterials with small osteoinductive moieties. Acta Biomater. 2013;9:8773–89.
55. Gilbert M, Giachelli CM, Stayton PS. Biomimetic peptides that engage specific integrin-dependent signaling pathways and bind to calcium phosphate surfaces. J Biomed Mater Res A. 2003;67:69–77.
56. Wang D, Mao J, Zhou B, Liao XF, Gong SQ, Liu Y, et al. A chimeric peptide that binds to titanium and mediates MC3T3-E1 cell adhesion. Biotechnol Lett. 2011;33:191–7.

How to cite this article: Biernat M, Ciołek L, Dzierżyńska M, et al. Porous chitosan/ZnO-doped bioglass composites as carriers of bioactive peptides. *Int J Appl Ceram Technol*. 2020;00:1–10. https://doi.org/10.1111/ijac.13609